On-Site Potential Creates Complexity in Systems with Disordered Coupling

I. Gershenzon,[1] B. Lacroix-A-Chez-Toine,[2,1] O. Raz,[1] E. Subag,[3] and O. Zeitouni[3]
[1]Department of Physics of Complex Systems, Weizmann Institute of Science, Rehovot 7610001, Israel
[2]Department of Mathematics, Kings College London, London WC2R 2LS, United Kingdom
[3]Department of Mathematics, Weizmann Institute of Science, Rehovot 76100, Israel

(Received 16 July 2022; accepted 4 April 2023; published 8 June 2023)

We calculate the average number of critical points $\bar{\mathcal{N}}$ of the energy landscape of a many-body system with disordered two-body interactions and a weak on-site potential. We find that introducing a weak nonlinear on-site potential dramatically increases $\bar{\mathcal{N}}$ to exponential in system size and give a complete picture of the organization of critical points. Our results extend solvable spin-glass models to physically more realistic models and are of relevance to glassy systems, nonlinear oscillator networks, and many-body interacting systems.

DOI: 10.1103/PhysRevLett.130.237103

Introduction.—The interplay between coupling, disorder, and nonlinearity is of interest in diverse areas of science. In physics, notable examples occur in spin and structural glasses [1–6], many-body localization [7,8], nonlinear wave propagation in disordered media [9–14], "dirty" superconductors [15,16], coupled oscillator networks [17–20], atomic spin gases [21,22], and in other systems [23–28]. Nonlinearity, coupling, and disorder are also commonly found in sociological models [29–31], epidemiology [32–36], ecological systems [37–39], computer science [40–43], and many other systems [44].

The energy of such disordered systems commonly exhibits a "rugged" landscape with a number of critical points that scales exponentially with system size. The abundance of critical points of certain energy and index is quantified in this Letter by the "complexity," i.e., the exponential scaling coefficient with system size [45] (sometimes referred to as the configurational entropy). This is defined as

$$\Sigma_k(E) = \lim_{N\to\infty} \frac{1}{N} \log \overline{\mathcal{N}_k(E)}, \tag{1}$$

where $\overline{\mathcal{N}_k(E)}$ is the disorder averaged density of critical points of index k at energy E. The geometry of a system's energy landscape, described by $\Sigma_k(E)$, was shown to directly influence static and dynamic properties of complex systems such as the mechanical properties of amorphous solids [46,47], the structure, function, and thermal properties of biomolecules [48], pinning properties of polymers to surfaces [49,50], the heat capacity of biomolecules [51], the relaxation timescales of glassy systems [52–56], the mobility in glass-forming liquids [57], and the transition rates between metastable states in complex systems [48,54,58]. In addition, the structure of rugged landscapes has a profound influence on optimization algorithms such as deep neural network training [40,59,60] and combinatorial optimization [43].

Early works used replica methods to derive approximate expressions for Σ in spin-glass models [1,2,55,61–64] and for disordered nonlinear optical systems [9,11]. Recently, rigorous random matrix methods were applied to count critical points in many models, including spin glasses [58,65–74], ecological systems [38], neural networks [42,75,76], and others [50,77].

Several works studied the complexity in confined disordered models, where a global confining potential term is added to a disordered energy landscape [65,66,72,78–80]. However, in many physical problems one is interested in coupled many-body systems with an on-site (nonlinear) potential. Notable systems where the local nonlinearity plays a central role alongside disordered coupling include amorphous solids [46,47,57], supefluidity, superconductivity, and Bose-Eienstein condensates (all modeled by the Gross-Pitaevskii equation) [15,23,24,81], wave propagation in nonlinear media [10,11], networks of coupled nonharmonic oscillators (optical, electrical, mechanical) [17,19,82], and models of conductors [83]. All these diverse systems share a common model energy structure: the coupling between degree of freedom (DOFs) is bilinear while the local ("on-site") potential energy is nonlinear.

In this Letter, we set out to study the complexity in this family of important models by analyzing a prototypical model with weak on-site nonlinearity (of general form) and disordered bilinear coupling. A central question motivating this study is the following. The bilinear form potential has at most N critical points, thus zero complexity. On the other hand, the limit of strong on-site potential can give rise to the Ising model with positive complexity [43]. It is therefore natural to ask, at which ratio between the two terms does the energy landscape become complex and what is the nature of this transition? We answer this question in the

regime of weak on-site potential by deriving a perturbative expression of the annealed complexity.

We find that in our model even a weak on-site term brings about positive complexity, with an exponential number of fixed points, i.e., a rugged energy landscape. We also find that the landscape of the system exhibits a qualitatively different critical point distribution in energy and index in comparison to the unperturbed model. Interestingly, the effect of adding an on-site potential resembles that of adding higher order interaction terms (as in the mixed p-spin model). We also find that an external magnetic field leads to a first order phase transition into a *trivial phase* with zero complexity (to leading order) and find the critical field. These results imply that disordered systems composed of coupled nonlinear units are expected to be found in a glassy phase exhibiting aging and memory in its dynamics, nontrivial response to external forces, as well as anomalous thermal properties. Technically, the calculations are facilitated by deriving a result on the disorder average of the modulus of the determinant of a sum of a GOE random matrix [79] and a small deterministic diagonal matrix [72].

The model analyzed in this Letter is defined by the energy landscape function $H(\sigma)$ [62]:

$$H(\sigma) = \sum_{i,j=1}^{N} J_{ij}\sigma_i\sigma_j + \kappa \sum_{i=1}^{N} u(\sigma_i) \equiv \phi(\sigma) + \kappa U(\sigma), \quad (2)$$

where $\sigma = (\sigma_1, \ldots, \sigma_N)$ is the vector whose components σ_i are continuous real valued "spin" DOFs constrained to the N-sphere, i.e., $\sum_i \sigma_i^2 = N$, J_{ij} is a random coupling matrix modeling disordered coupling, $u(\sigma_i)$ is a deterministic on-site nonlinear potential (with bounded derivatives), and κ is the deterministic potential strength. Note that in this model the number of critical points is invariant to global shifts in $u(x)$ as well as to addition of quadratic terms (which are constant on the N-sphere). In this Letter, we fix the definition of $u(x)$ by assuming that the Gaussian weighted average of u and u'' is zero. The stochastic part of H is denoted by $\phi(\sigma)$ and the deterministic part by $\kappa U(\sigma)$. We choose the coupling matrix J to be distributed according to the Gaussian orthogonal ensemble [84]—a disordered mean-field coupling. This choice along with the spherical constraints allows for the identification of the coupling term in H with the 2-spin spherical model [67].

To evaluate the average total number of critical points $\overline{\mathcal{N}_{\text{tot}}}$ of the model, we use the Kac-Rice formula on the sphere (as given in Ref. [67]):

$$\overline{\mathcal{N}_{\text{tot}}} = \int_{\sqrt{N}\mathbb{S}^{N-1}} d\sigma_{N-1}\, \overline{|\det(\nabla^2 H)|\delta(\nabla H)}, \quad (3)$$

where ∇H and $\nabla^2 H$ are the covariant derivative and Hessian matrix of H on the sphere, respectively. In what follows we evaluate the annealed total complexity Σ_{tot} defined similarly to Eq. (1) in the perturbative regime of weak on-site potential, i.e., $\kappa \ll 1$.

Main results.—In this section we cite the results for the total annealed complexity Σ_{tot}, and the annealed complexity of fixed extensive index $k = Na$ (number of negative eigenvalues of the Hessian) and extensive energy $E = \epsilon N$, $\Sigma_a(\epsilon)$ as a functional of the potential $u(x)$. The complexity Σ_{tot} is found to be

$$\Sigma_{\text{tot}}[u] = \kappa^2 \max(0, \Theta[u]) + O(\kappa^3), \quad (4)$$

with

$$\Theta[u] = \frac{1}{4}\int dx \frac{e^{-x^2/2}}{\sqrt{2\pi}} [u''(x)^2 - u'(x)^2]. \quad (5)$$

We see that the complexity is second order in κ and has two distinct solution branches. To leading order, the complexity is zero in the first branch, and is $\Theta[u]$ in the other branch. The total complexity of the system is the maximum of these two. The potential $u(x)$ dictates the sign of $\Theta[u]$ and consequently which branch dominates. We show that $\Theta[u] > 0$ for any potential with $u'(0) = 0$, i.e., without an external field component [see Supplemental Material (SM) [85]]. Thus, addition of a weak generic anharmonic potential brings about an exponential number of critical points for any nonzero magnitude (a phase transition at zero). Also, we see that the relation of the complexity with the nonlinearity strength does not depend on the details of the potential but only on the number $\Theta[u]$. We defer the discussion on the case $\Theta[u] < 0$ to the section on response to an external field (below).

Next, to gain further insight about the geometry of the landscape of our model, we calculate the complexity of critical points with a given index $k = aN$ and a given energy $E = \epsilon N$. This is found to be (see SM [85])

$$\Sigma_a(\epsilon)[u] = \kappa^2\left(1 - \frac{\eta^2(a)}{4}\right)\Theta[u] - \frac{\kappa^2}{2}\left\{\frac{1}{\kappa^2}[\eta(a) - \epsilon\sqrt{2}] + \eta(a)\tilde{\Delta}\right\}^2 + O(\kappa^3), \quad (6)$$

where $\tilde{\Delta}$ is a functional of $u(x)$ which is defined in the SM. $\eta(a)$ is the solution of

$$\frac{1}{2\pi}\int_{-2}^{\eta(a)} dx\sqrt{4 - x^2} = a. \quad (7)$$

Note that this expression is valid when $\eta(a) - \epsilon\sqrt{2} = O(\kappa^2)$ where outside this range the complexity is highly negative; i.e., the average number of critical points is exponentially negligible (see SM). The dependence of $\Sigma_a(\epsilon)$, to leading order in κ, on the index a and the energy ϵ is plotted in Fig. 1 where it is seen that critical points with

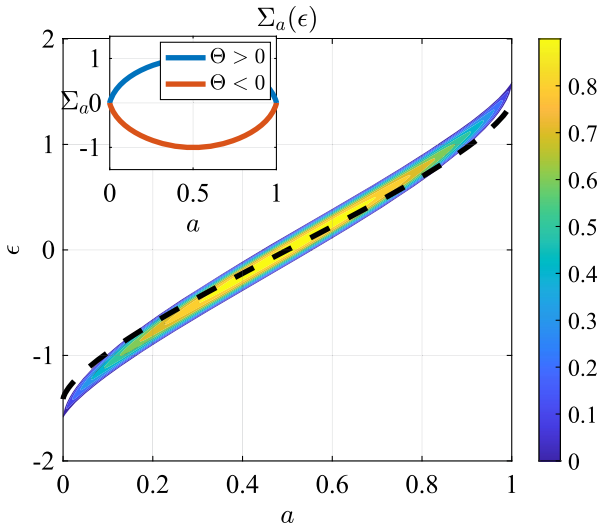

FIG. 1. The complexity of critical points of a given index and energy $\Sigma_a(\epsilon)$ as a function of the normalized index $a = k/N$ and energy $\epsilon = E/N$ for $\Theta = 1$, $\tilde{\Delta} = 3$ [corresponding to $u(x) = \frac{4}{9}x^3$] and $\kappa = 0.2$. Dashed line: relation between ϵ and a in the unperturbed 2-spin model. Inset: the complexity Σ_a for a given index $k = aN$. The values are normalized to the maximal value. In blue, Σ_a is the plotted versus a in the case where $\Theta[u]$ is positive. In red, we depict the case where $\Theta[u]$ is negative.

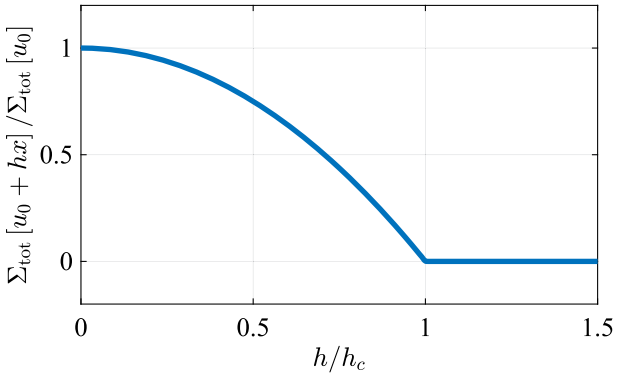

FIG. 2. The complexity $\Sigma_{\rm tot}$ second order correction as a function of the magnetic field strength, scaled by the critical strength, for the case of an on-site potential with $\overline{u_0'} = 0$.

positive complexity are narrowly concentrated around a line in the $a\epsilon$ plane defined by

$$\epsilon = \frac{\eta(a)}{\sqrt{2}}(1 + \kappa^2\tilde{\Delta}). \tag{8}$$

This tight connection between energy and index is also found in other models [41,45,68] as well as in the unperturbed model. However, in the unperturbed case only critical points obeying $\epsilon = \eta(a)/\sqrt{2}$ exist and the probability to find other critical points vanishes like $O[\exp(-N^2)]$ [67]. Thus the on-site potential serves to broaden the distribution of critical points to include an exponential number of critical points outside the above relation. We also see that the on-site potential shifts by $O(\kappa^2)$ the concentration line of critical points. This broadening and shift is similar to what occurs in the transition from pure p-spin models to mixed p-spin models. This is expected to have a profound effect on the relaxation dynamics as described in Ref. [53]. In addition, we see that critical points of index $k = N/2$ and zero energy have the highest complexity. The marginal distribution of the complexity versus the index is depicted in the inset of Fig. 1. We see that saddle points of extensive index become exponentially abundant while the number of critical points with $\lim_{N\to\infty} k/N = 0$ does not change on the exponential scale]. Moreover, we show in the SM (Sec. V A) that the expected number of maxima and minima does not change as well [85]. This increase in saddles makes the landscape between minima rugged with additional barriers [58]. This is expected to have implications on the lifetime of metastable states as well as relaxation pathways [54]. We also note that the distribution of critical points in the regime of weak nonlinearity is universal in that it does not depend on the details of $u(x)$ but only on "macroscopic" functionals of $u(x)$ (Θ and $\tilde{\Delta}$).

As an illustrating example, let us consider the specific example of a network of coupled optical oscillators (lasers [19] or degenerate optical parametric oscillators [18]). In these systems the coupling between oscillators is typically bilinear while the on-site potential's form and strength depend on an external driving (pumping): For zero or weak driving the on-site potential is harmonic (and thus trivial) while increasing the drive adds an anharmonic term to the potential which can lead to a pitchfork bifurcation resulting in bistability. The experimental realization of large systems of this sort and their use to simulate spin models as well as heuristic machines for optimization has led to an interest in their dynamics in various regimes [86–88]. Our results indicate that the energy landscape of these systems becomes rugged and complex even slightly above the system's oscillation threshold where the nonlinearity is weak. This means that the dynamics of these systems are expected to be nontrivial in this regime as well and to become more so as the nonlinearity is further increased.

Response to external field.—As shown in Appendix D of the SM [85], a strong enough external field $h = u'(0)$ leads to negative $\Theta[u]$ [see Eq. (5)]. In this case the complexity is zero to leading order and our results are similar to those in Refs. [78,80] where "trivial topology" of the landscape was found under a sufficiently strong external magnetic field. In the trivial topology phase, the energy landscape has only two critical points (a minimum and a maximum) [80]. Our results for the complexity of a given index Σ_a as depicted in the inset of Fig. 1, in this case, are consistent with this picture: the complexity is non-negative only for indices $k = o(N)$ [or $k = N - o(N)$], which represent critical points that are a minimum (maximum) in most directions. From the perspective of the spin value distribution, we show

[see Eq. (59) in SM] that the distribution is skewed in the direction of the applied magnetic field, such that for $u(x) = hx$ this leads to an $O(\kappa)$ shift in the disorder averaged magnetization $\bar{\sigma} \sim \kappa h$. This shift directly shows the alignment of the spins along the external field at the maxima or minima of the model.

Having explored both system states, we now turn to discussing the transition between them. We now show that, driving the system between the states can be achieved by changing the magnetic field strength $u'(0)$, see Fig. 2. Assume that for a specific potential $u_0(x)$ the added complexity $\Theta[u_0]$ is positive, e.g., any potential with $u_0'(0) = 0$. Next, we add an external field of strength h such that $u(x) = u_0(x) + hx$. A simple calculation shows:

$$\Theta[u] = \Theta[u_0] - \frac{h^2}{4} - \frac{h}{2}\overline{u'}, \tag{9}$$

where $\overline{u(x)}$ denotes averaging the weighted average of $u(x)$ with respect to the standard Gaussian distribution. It is seen that for large enough field strength, i.e., $h > h_{c+}$ or $h < h_{c-}$, $\Theta[u]$ drops below zero. At h_c there is a transition to the zero complexity branch. h_c is found by equating the above expression to zero:

$$h_{c\pm} = \pm\sqrt{\overline{u'} + 4\Theta[u_0]} - \overline{u'}. \tag{10}$$

It is also seen that the form of this transition is independent of the form of $u_0(x)$.

Although our main motivation is to analyze perturbations of the 2-spin spherical model, the same analysis can be readily applied for a general p-spin spherical model. The average total complexity $\Sigma_{\mathrm{tot}}^{(p>2)}$ reads in that case:

$$\Sigma_{\mathrm{tot}}^{(p>2)}[u] = \frac{1}{2}\log(p-1) + \kappa^2\Theta^{(p)}[u] + O(\kappa^3), \tag{11}$$

where $\Theta^{(p)}[u]$ appears in Eq. (9) of the SM [85]. Note that the unperturbed complexity is consistent with Ref. [67]. As in the 2-spin spherical model, the correction to the total complexity for the p-spin model is $O(\kappa^2)$. However, there is only a single solution branch and the total complexity is always positive (in the regime of weak κ). Moreover, the on-site potential can either increase or decrease the total complexity depending on its form, in contrast to the 2-spin spherical model, where it can only be increased. Specifically, we also recover the results of Ref. [80] in the regime of small external magnetic field. In Eq. (9) of the SM we also provide an expression for the complexity $\Sigma_a^{(p>2)}[u]$ of the p-spin model with extensive fixed index $k = Na$ for any integer p.

Derivation outline.—The full derivation of our results is quite lengthy and technical. We therefore provide only the outline of the calculation of the complexity defined in Eq. (1) for the $p = 2$ case. The full derivation for this and other cases is given in the SM [85]. We start the calculation of Eq. (3) by evaluating the disorder average $\overline{|\det(\nabla^2 H)|\delta(\nabla H)}$ at a fixed position σ on the sphere. The average is taken over the joint distribution of the covariant Hessian and gradient of $\phi(\sigma)$. First, we use the independence of $\nabla\phi$ and $\nabla\phi^2$ to factor out the expectation as follows:

$$\overline{|\det(\nabla^2 H)|\delta(\nabla H)} = \overline{\delta(\nabla H)}\,\overline{|\det(\nabla^2 H)|}. \tag{12}$$

To evaluate the expectation values in Eq. (12) we start by writing the distribution of the random matrix $\nabla^2\phi$ and $\nabla\phi$ (see SM, Appendix A). Equipped with this probability density function, the integral $\overline{\delta(\nabla H)}$ is easily carried out to give

$$\overline{\delta[\nabla H(\sigma)]} = \left(\frac{1}{2\pi p}\right)^{N/2} \exp\left(-\frac{\kappa^2}{2p}\|\nabla U(\sigma)\|^2\right). \tag{13}$$

The evaluation of $\overline{|\det\nabla^2 H(\sigma)|}$ is more involved and constitutes the main technical contribution of this Letter. The challenge is due to $\nabla^2 H$ being a sum of noncommuting matrices: the random matrix $\nabla^2\phi$ and the diagonal deterministic matrix $\kappa\nabla^2 U$ (see SM for explicit expressions). We address this difficulty by resorting to a perturbative evaluation of the eigenvalue distribution of $\nabla^2 H$ in the small κ regime. This distribution is used in turn to calculate the determinant modulus as described below.

To evaluate $\overline{|\det\nabla^2 H(\sigma)|}$ we use recent results (Proposition 5.3 in Ref. [72], Theorem 4.1 in Ref. [89]) to formally express the expectation value in terms of the eigenvalue distributions of $\nabla^2\phi$ and $\kappa\nabla^2 U$:

$$\lim_{N\to\infty}\frac{1}{N}\log\overline{|\det\nabla^2 H(\sigma)|} = \sup_s \int d\lambda \nu_{\nabla^2 H(\sigma)}(\lambda) \times \log|\lambda - s| - \frac{s^2}{2p^2}, \tag{14}$$

where $\nu_{\nabla^2 H(\sigma)}$ is the eigenvalue distribution of $\nabla^2 H(\sigma)$. This distribution, in the limit of large N, converges to the free convolution, denoted $\boxplus$, of the eigenvalue distributions of $\nabla^2\phi$ and $\kappa\nabla^2 U$ [72,84],

$$\nu_{\nabla^2 H}(\lambda) = (\rho_{\mathrm{sc}} \boxplus \nu_{\kappa\nabla^2 U})(\lambda), \tag{15}$$

where $\nu_{\kappa\nabla^2 U}(\lambda)$ is the eigenvalue distribution of $\kappa\nabla^2 U$ and $\rho_{\mathrm{sc}}(\lambda)$ is the Wigner semicircle distribution with variance $V_p \equiv p(p-1)$:

$$\rho_{\mathrm{sc}}(\lambda) = \frac{1}{2\pi V_p}\sqrt{4V_p - \lambda^2}. \tag{16}$$

Intuitively, the free convolution is the random matrix analog to the convolution operation used to calculate the probability density of a sum of independent random

variables. It is nonlinear and generally the result cannot be expressed in a closed form. However, in the regime of small κ we are able to find a perturbative expression for $\nu_{\nabla^2 H}(\lambda)$ by solving perturbatively the Pastur integral equation [90]. This results, up to $O(\kappa^3)$, in a shifted and widened semicircular distribution given by

$$\nu_{\nabla^2 H}(\lambda) = \frac{1}{\sqrt{1+\kappa^2 V_{\nabla^2 U}}} \rho_{\mathrm{sc}}\left(\frac{\lambda - \kappa\sqrt{V_p} m_{\nabla^2 U}}{\sqrt{1+\kappa^2 V_{\nabla^2 U}}}\right) + O(\kappa^3), \tag{17}$$

with $m_{\nabla^2 U}$ and $V_{\nabla^2 U}$ the mean and variance of the eigenvalue distribution of $(1/\sqrt{V_p})\nabla^2 U$, respectively. Now we can proceed to derive a closed form expression for $\overline{|\det(\nabla^2 H)|}$ by substitution of the above expression for $\nu_{\nabla^2 H}(\lambda)$ in Eq. (14) and optimization with respect to s:

$$\begin{aligned} &\lim_{N\to\infty} \frac{1}{N} \log \overline{|\det \nabla^2 H(\sigma)|} \\ &= \frac{1}{2}(-1 + \log 2) - \frac{1}{4}\kappa^2 m_{\nabla^2 U}^2 \\ &\quad + \kappa^2 V_{\nabla^2 U} \begin{cases} |\eta_2| - \frac{1}{2} & |\eta_2(\sigma)| \geq 2 \\ \frac{1}{2} + \frac{1}{4}\eta_2^2 & |\eta_2(\sigma)| < 2, \end{cases} \end{aligned} \tag{18}$$

where we ignored terms which are $O(\kappa)^3$ and $\eta_2 = [(m_{\nabla^2 U}/\kappa)/V_{\nabla^2 U}]$. Note that the result contains two branches. The form of the supremum equation and its solution branches is similar to the one found in Ref. [80] as was discussed in detail following the results statement in the previous section.

Now we turn to the evaluation of the integration over the N-sphere in Eq. (3):

$$\overline{\mathcal{N}_{\mathrm{tot}}} = \left(\frac{1}{2\pi p}\right)^{N/2} \int_{\mathbb{S}^{N-1}} d\sigma \, \exp\left(-\frac{\kappa^2}{2p}\|\nabla U\|^2\right) \overline{|\det \nabla^2 H|}. \tag{19}$$

The approach we adopt for the evaluation of this integral is to pass from spatial integration over the surface of the sphere to functional integration over the empirical distribution of σ_i (the "Coulomb gas" technique [91]). This results in a functional optimization problem whose formulation and perturbative solution are described in detail in the SM, Sec. IV D [85].

Discussion.—We found that introducing an "on-site" nonlinearity to a disordered mean-field coupled system can significantly increase the complexity of the energy landscape of the system. We characterized the changes to the geometry of the energy landscape through the distribution of critical points with respect to energy and index and found them to exhibit a universal behavior independent of the specifics of the added nonlinearity. These results are immediately applicable to the characterization of the energy landscape of physical systems with on-site weak nonlinearity and disordered long-range coupling such as "soft-spin" glass models [1,2,55,61], coupled oscillator networks [17–19], and atomic spin gases [21].

Future research directions include extending the results of this Letter beyond the perturbative regime, relaxation of the spherical constraint to study more diverse physical models, studying the quenched complexity, possibly by carrying out a second moment analysis [69]. Also, it is of interest to consider short-range coupling schemes possibly by considering banded random matrix models [72,92].

O. R. is supported by the Abramson Family Center for Young Scientists, the Israel Science Foundation Grant No. 950/19, and by the Minerva foundation. I. G. is grateful to Amy Entin for her help with writing this manuscript. B. L.-A-C.-T. is supported by the EPSRC Grant No. EP/V002473/1 Random Hessians and Jacobians: theory and applications. O. Z. was partially supported by the European Research Council (ERC) under the European Union's Horizon 2020 research and innovation programme (Grant Agreement No. 692452) and by the Israel Science Foundation Grant No. 421/20. E. S. is supported by the Israel Science Foundation Grant No. 2055/21 and the Skirball Chair in New Scientists.

[1] T. Castellani and A. Cavagna, Spin-glass theory for pedestrians, J. Stat. Mech. (2005) 215.
[2] M. Mézard, G. Parisi, and M. Virasoro, *Spin Glass Theory and Beyond: An Introduction to the Replica Method and Its Applications* (World Scientific Publishing Company, Singapore, 1987), Vol. 9.
[3] H. T. Diep, *Frustrated Spin Systems*, 2nd ed. (World Scientific Publishing Co., Singapore, 2013), pp. 1–617.
[4] L. Gartner and E. Lerner, Nonlinear modes disentangle glassy and Goldstone modes in structural glasses, SciPost Phys. **1**, 016 (2016).
[5] E. A. Goremychkin, R. Osborn, B. D. Rainford, R. T. MacAluso, D. T. Adroja, and M. Koza, Spin-glass order induced by dynamic frustration, Nat. Phys. **4**, **766** (2008).
[6] K. Kim, M. S. Chang, S. Korenblit, R. Islam, E. E. Edwards, J. K. Freericks, G. D. Lin, L. M. Duan, and C. Monroe, Quantum simulation of frustrated Ising spins with trapped ions, Nature (London) **465**, 590 (2010).
[7] K. S. Tikhonov and A. D. Mirlin, From Anderson localization on random regular graphs to many-body localization, Ann. Phys. (Amsterdam) **435**, 168525 (2021).
[8] D. A. Abanin, E. Altman, I. Bloch, and M. Serbyn, Colloquium: Many-body localization, thermalization, and entanglement, Rev. Mod. Phys. **91**, 021001 (2019).
[9] F. Antenucci, A. Crisanti, and L. Leuzzi, Complex spherical $2+4$ spin glass: A model for nonlinear optics in random media, Phys. Rev. A **91**, 053816 (2015).
[10] A. Zyuzin and B. Spivak, Propagation of nonlinear waves in disordered media, J. Opt. Soc. Am. B **21**, 177 (2004).

[11] C. Conti and L. Leuzzi, Complexity of waves in nonlinear disordered media, Phys. Rev. B **83**, 134204 (2011).
[12] N. Ghofraniha, I. Viola, F. Di Maria, G. Barbarella, G. Gigli, L. Leuzzi, and C. Conti, Experimental evidence of replica symmetry breaking in random lasers, Nat. Commun. **6**, 6058 (2015).
[13] S. W. Shaw and C. Pierre, Normal modes for non-linear vibratory systems, J. Sound Vib. **164**, 85 (1993).
[14] S. Fishman, Y. Krivolapov, and A. Soffer, The nonlinear Schrödinger equation with a random potential: Results and puzzles, Nonlinearity **25**, R53 (2012).
[15] T. R. Kirkpatrick and D. Belitz, Suppression of Superconductivity by Disorder, Phys. Rev. Lett. **68**, 3232 (1992).
[16] D. S. Fisher, M. P. A. Fisher, and D. A. Huse, Thermal fluctuations, quenched disorder, phase transitions, and transport in type-II superconductors, Phys. Rev. B **43**, 130 (1991).
[17] T. Inagaki, Y. Haribara, K. Igarashi, T. Sonobe, S. Tamate, T. Honjo, A. Marandi, P. L. McMahon, T. Umeki, K. Enbutsu, O. Tadanaga, H. Takenouchi, K. Aihara, K. I. Kawarabayashi, K. Inoue, S. Utsunomiya, and H. Takesue, A coherent Ising machine for 2000-node optimization problems, Science **354**, 603 (2016).
[18] Z. Wang, A. Marandi, K. Wen, R. L. Byer, and Y. Yamamoto, Coherent Ising machine based on degenerate optical parametric oscillators, Phys. Rev. A **88**, 063853 (2013).
[19] M. Nixon, E. Ronen, A. A. Friesem, and N. Davidson, Observing Geometric Frustration with Thousands of Coupled Lasers, Phys. Rev. Lett. **110**, 184102 (2013).
[20] S. Gopalakrishnan, B. L. Lev, and P. M. Goldbart, Frustration and Glassiness in Spin Models with Cavity-Mediated Interactions, Phys. Rev. Lett. **107**, 277201 (2011).
[21] Y. Horowicz, O. Katz, O. Raz, and O. Firstenberg, Critical dynamics and phase transition of a strongly interacting warm spin gas, Proc. Natl. Acad. Sci. U.S.A. **118**, e2106400118 (2021).
[22] C. Lippe, T. Klas, J. Bender, P. Mischke, T. Niederprüm, and H. Ott, Experimental realization of a 3D random hopping model, Nat. Commun. **12**, 6976 (2021).
[23] C. Fort, L. Fallani, V. Guarrera, J. E. Lye, M. Modugno, D. S. Wiersma, and M. Inguscio, Effect of Optical Disorder and Single Defects on the Expansion of a Bose-Einstein Condensate in a One-Dimensional Waveguide, Phys. Rev. Lett. **95**, 170410 (2005).
[24] P. Lugan, D. Clément, P. Bouyer, A. Aspect, M. Lewenstein, and L. Sanchez-Palencia, Ultracold Bose Gases in 1D Disorder: From Lifshits Glass to Bose-Einstein Condensate, Phys. Rev. Lett. **98**, 170403 (2007).
[25] D. C. Tsui, Nobel lecture: Interplay of disorder and interaction in two-dimensional electron gas in intense magnetic fields, Rev. Mod. Phys. **71**, 891 (1999).
[26] D. G. Joshi, C. Li, G. Tarnopolsky, A. Georges, and S. Sachdev, Deconfined Critical Point in a Doped Random Quantum Heisenberg Magnet, Phys. Rev. X **10**, 021033 (2020).
[27] J. C. Eilbeck, P. S. Lomdahl, and A. C. Scott, The discrete self-trapping equation, Physica (Amsterdam) **16D**, 318 (1985).
[28] M. Goldstein, Viscous liquids and the glass transition: A potential energy barrier picture, J. Chem. Phys. **51**, 3728 (1969).
[29] A. Namatame and S.-H. Chen, *Agent-Based Modeling and Network Dynamics* (Oxford University Press, New York, 2016).
[30] G. Palla, A. L. Barabási, and T. Vicsek, Community dynamics in social networks, Fluctuation Noise Lett. **7**, L273 (2007).
[31] H. Ebel, J. Davidsen, and S. Bornholdt, Dynamics of social networks, Complexity **8**, 24 (2002).
[32] L. Sattenspiel and K. Dietz, A structured epidemic model incorporating geographic mobility among regions, Math. Biosci. **128**, 71 (1995).
[33] R. Pastor-Satorras, C. Castellano, P. Van Mieghem, and A. Vespignani, Epidemic processes in complex networks, Rev. Mod. Phys. **87**, 925 (2015).
[34] F. Fu, D. I. Rosenbloom, L. Wang, and M. A. Nowak, Imitation dynamics of vaccination behaviour on social networks, Proc. R. Soc. B **278**, 42 (2011).
[35] A. W. Roddam, Mathematical epidemiology of infectious diseases: Model building, analysis and interpretation, Int. J. Epidemiol. **30**, 186 (2001).
[36] H. W. Hethcote, Mathematics of infectious diseases, SIAM Rev. **42**, 599 (2000).
[37] R. M. May, *Stability and Complexity in Model Ecosystems*, Princeton Landmarks In Biology (Princeton University Press, Princeton, NJ, 2001).
[38] Y. V. Fyodorov and B. A. Khoruzhenko, Nonlinear analogue of the May-Wigner instability transition, Proc. Natl. Acad. Sci. U.S.A. **113**, 6827 (2016).
[39] S. Allesina and S. Tang, The stabilitycomplexity relationship at age 40: A random matrix perspective, Popul. Ecol. **57**, 63 (2015).
[40] Y. Bahri, J. Kadmon, J. Pennington, S. S. Schoenholz, J. Sohl-Dickstein, and S. Ganguli, Statistical mechanics of deep learning, Annu. Rev. Condens. Matter Phys. **11**, 501 (2020).
[41] M. Baity-Jesi, L. Sagun, M. Geiger, S. Spigler, G. Ben Arous, C. Cammarota, Y. Lecun, M. Wyart, and G. Biroli, Comparing dynamics: Deep neural networks versus glassy systems, J. Stat Mech. (2019) 124013.
[42] S. Becker, Y. Zhang, and A. A. Lee, Geometry of Energy Landscapes and the Optimizability of Deep Neural Networks, Phys. Rev. Lett. **124**, 108301 (2020).
[43] M. Mézard and A. Montanari, *Information, Physics, and Computation* (Oxford University Press, Oxford, 2009).
[44] M. E. Newman, A. L. Barabási, and D. J. Watts, *The Structure and Dynamics of Networks* (Princeton University Press, Princeton, NJ, 2011).
[45] A. J. Bray and D. S. Dean, Statistics of Critical Points of Gaussian Fields on Large-Dimensional Spaces, Phys. Rev. Lett. **98**, 150201 (2007).
[46] E. Bouchbinder, E. Lerner, C. Rainone, P. Urbani, and F. Zamponi, Low-frequency vibrational spectrum of mean-field disordered systems, Phys. Rev. B **103**, 174202 (2021).
[47] Y. Jin and H. Yoshino, Exploring the complex free-energy landscape of the simplest glass by rheology, Nat. Commun. **8**, 1 (2017).
[48] L. Milanesi, J. P. Waltho, C. A. Hunter, D. J. Shaw, G. S. Beddard, G. D. Reid, S. Dev, and M. Volk, Measurement of

energy landscape roughness of folded and unfolded proteins, Proc. Natl. Acad. Sci. U.S.A. **109**, 19563 (2012).
[49] Y. V. Fyodorov, P. L. Doussal, A. Rosso, and C. Texier, Exponential number of equilibria and depinning threshold for a directed polymer in a random potential, Ann. Phys. (Amsterdam) **397**, 1 (2018).
[50] Y. V. Fyodorov and P. Le Doussal, Manifolds in a high-dimensional random landscape: Complexity of stationary points and depinning, Phys. Rev. E **101**, 020101 (2020).
[51] M. Goldstein, Viscous liquids and the glass transition. V. Sources of the excess specific heat of the liquid, J. Chem. Phys. **64**, 4767 (1976).
[52] Y. Nishikawa, M. Ozawa, A. Ikeda, P. Chaudhuri, and L. Berthier, Relaxation Dynamics in the Energy Landscape of Glass-Forming Liquids, Phys. Rev. X **12**, 021001 (2022).
[53] G. Folena, S. Franz, and F. Ricci-Tersenghi, Rethinking Mean-Field Glassy Dynamics and Its Relation with the Energy Landscape: The Surprising Case of the Spherical Mixed p-Spin Model, Phys. Rev. X **10**, 031045 (2020).
[54] T. Rizzo, Path integral approach unveils role of complex energy landscape for activated dynamics of glassy systems, Phys. Rev. B **104**, 094203 (2021).
[55] A. Cavagna, I. Giardina, and G. Parisi, Role of saddles in mean-field dynamics above the glass transition, J. Phys. A **34**, 5317 (2001).
[56] U. Buchenau, Energy landscape—A key concept in the dynamics of liquids and glasses, J. Phys. Condens. Matter **15**, 5955 (2003).
[57] P. Charbonneau, J. Kurchan, G. Parisi, P. Urbani, and F. Zamponi, Fractal free energy landscapes in structural glasses, Nat. Commun. **5**, 1 (2014).
[58] V. Ros, G. Biroli, and C. Cammarota, Complexity of energy barriers in mean-field glassy systems, Europhys. Lett. **126**, 20003 (2019).
[59] Y. N. Dauphin, R. Pascanu, C. Gulcehre, K. Cho, S. Ganguli, and Y. Bengio, Identifying and attacking the saddle point problem in high-dimensional non-convex optimization, in *Proc. Advances in Neural Information Processing Systems* (2014), Vol. 4, https://proceedings.neurips.cc/paper/2014/hash/17e23e50bedc63b4095e3d8204ce063b-Abstract.html.
[60] S. Becker, Y. Zhang, and A. A. Lee, Geometry of Energy Landscapes and the Optimizability of Deep Neural Networks, Phys. Rev. Lett. **124**, 108301 (2020).
[61] A. Cavagna, I. Giardina, and G. Parisi, Stationary points of the Thouless-Anderson-Palmer free energy, Phys. Rev. B **57**, 11251 (1998).
[62] M. L. Rosinberg and T. Munakata, Hysteresis and complexity in the mean-field random-field Ising model: The soft-spin version, Phys. Rev. B **79**, 174207 (2009).
[63] J. Kurchan, Replica trick to calculate means of absolute values: Applications to stochastic equations, J. Phys. A **24**, 4969 (1991).
[64] R. Monasson, Structural Glass Transition and the Entropy of the Metastable States, Phys. Rev. Lett. **75**, 2847 (1995).
[65] Y. V. Fyodorov, Complexity of Random Energy Landscapes, Glass Transition, and Absolute Value of the Spectral Determinant of Random Matrices, Phys. Rev. Lett. **92**, 240601 (2004).
[66] Y. V. Fyodorov and I. Williams, Replica symmetry breaking condition exposed by random matrix calculation of landscape complexity, J. Stat. Phys. **129**, 1081 (2007).
[67] A. Auffinger, G. Ben Arous, and J. Černý, Random matrices and complexity of spin glasses, Commun. Pure Appl. Math. **66**, 165 (2013).
[68] A. Auffinger and G. Ben Arous, Complexity of random smooth functions on the high-dimensional sphere, Ann. Probab. **41**, 4214 (2013).
[69] E. Subag, The complexity of spherical p-spin models—A second moment approach, Ann. Probab. **45**, 3385 (2017).
[70] B. McKenna, Non-invariant random matrices and landscape complexity, Ph.D. thesis, New York University, 2021.
[71] B. McKenna, Complexity of bipartite spherical spin glasses, arXiv:2105.05043.
[72] G. B. Arous, P. Bourgade, and B. McKenna, Landscape complexity beyond invariance and the elastic manifold, arXiv:2105.05051.
[73] E. Subag, The free energy of spherical pure p-spin models—Computation from the TAP approach, arXiv:2101.04352.
[74] E. Subag, Free energy landscapes in spherical spin glasses, arXiv:1804.10576.
[75] A. Choromanska, M. Henaff, M. Mathieu, G. Ben Arous, and Y. LeCun, The loss surfaces of multilayer networks. Proceedings of the eighteenth international conference on artificial intelligence and statistics, Proc. Mach. Learn. Res. **38**, 192 (2015), https://proceedings.mlr.press/v38/choromanska15.html.
[76] A. Maillard, G. B. Arous, and G. Biroli, Landscape complexity for the empirical risk of generalized linear models, Proc. Mach. Learn. Res. **107**, 287 (2020), https://proceedings.mlr.press/v107/maillard20a.html.
[77] B. Lacroix-A-Chez-Toine and Y. V. Fyodorov, Counting equilibria in a random non-gradient dynamics with heterogeneous relaxation rates, J. Phys. A **55**, 144001 (2022).
[78] Y. V. Fyodorov and P. Le Doussal, Topology trivialization and large deviations for the minimum in the simplest random optimization, J. Stat. Phys. **154**, 466 (2014).
[79] A. Dembo and O. Zeitouni, Matrix optimization under random external fields, J. Stat. Phys. **159**, 1306 (2015).
[80] D. Belius, J. Černý, S. Nakajima, and M. A. Schmidt, Triviality of the geometry of mixed p-spin spherical Hamiltonians with external field, J. Stat. Phys. **186**, 12 (2022).
[81] B. Shapiro, Cold atoms in the presence of disorder, J. Phys. A **45**, 143001 (2012).
[82] F. Caravelli, Asymptotic behavior of memristive circuits, Entropy **21**, 789 (2019).
[83] G. Tarnopolsky, C. Li, D. G. Joshi, and S. Sachdev, Metal-insulator transition in a random Hubbard model, Phys. Rev. B **101**, 205106 (2020).
[84] G. W. Anderson, A. Guionnet, and O. Zeitouni, *An Introduction to Random Matrices* (Cambridge University Press, Cambridge, England, 2009).
[85] See Supplemental Material at http://link.aps.org/supplemental/10.1103/PhysRevLett.130.237103 for detailed result derivation.

[86] K. Tatsumura, Large-scale combinatorial optimization in real-time systems by FPGA-based accelerators for simulated bifurcation, in *Proceedings of the 11th International Symposium on Highly Efficient Accelerators and Reconfigurable Technologies (HEART '21)* (Association for Computing Machinery, New York, 2021).

[87] T. Inagaki, K. Inaba, R. Hamerly, K. Inoue, Y. Yamamoto, and H. Takesue, Large-scale ising spin network based on degenerate optical parametric oscillators, Nat. Photonics **10**, 415 (2016).

[88] F. Böhm, T. Inagaki, K. Inaba, T. Honjo, K. Enbutsu, T. Umeki, R. Kasahara, and H. Takesue, Understanding dynamics of coherent Ising machines through simulation of large-scale 2D Ising models, Nat. Commun. **9**, 1 (2018).

[89] G. Ben Arous, P. Bourgade, and B. McKenna, Exponential growth of random determinants beyond invariance, Probab. Math. Phys. **3**, 731 (2022).

[90] P. Biane, On the free convolution with a semi-circular distribution, Indiana Univ. Math. J. **46**, 705 (1997).

[91] F. J. Dyson, Statistical theory of the energy levels of complex systems. I, J. Math. Phys. (N.Y.) **3**, 140 (1962).

[92] P. Bourgade, L. Erdős, H. T. Yau, and J. Yin, Universality for a class of random band matrices, Adv. Theor. Math. Phys. **21**, 739 (2017).